

IJEAST

INTERNATIONAL JOURNAL
OF ENGINEERING APPLIED SCIENCE
AND TECHNOLOGY

VOLUME : 1 ISSUE : 10 Print / Issue Publication Date: 10-Oct-2016

ISSN : 2455-2143

Indexed In

Google SCHOLAR OPEN ACCESS doi Crossref

WWW.IJEAST.COM

editor@ijeast.com

International Journal of Engineering Applied Sciences and Technology, 2016
Vol. 1, Issue 10, ISSN No. 2455-2143, Pages 103-109
Published Online August - September 2016 in IJEAST (http://www.ijeast.com)



PREPARATION, CHARACTERIZATION AND PHOTOCATALYTIC ACTIVITY OF LEAF LIKE α-IRON OXIDE-REDUCED GRAPHENE OXIDE COMPOSITE

Balaji Anjaneyulu Rachuri, Parasuram Naidu Gongada, Muralikrishna Rallabhandi
Department of Physical, Nuclear chemistry and Chemical Oceanography,
Andhra University, India

Sathish Mohan Botsa
Department of Inorganic and analytical chemistry,
Andhra University, India

Abstract: A composite of reduced graphene oxide supported leaf like α-Fe_2O_3 has been fabricated through a simple hydrothermal method. The structural and morphological characterizations of the as-prepared composites were carried out using X-ray Diffraction, Fourier Transform Infrared spectra, Scanning Electron Microscopy, Energy Dispersive X-ray spectroscopy, Thermogravimetry analysis, UV-vis/DRS spectrophotometer and BET data. Leaf like α-Fe_2O_3-rGO exhibited superior photocatalytic activity than leaf like α-Fe_2O_3 for the degradation of Brilliant green (BG) and Acetophenone (AP) in an aqueous solution under visible light. The showing impressive photocatalytic enhancements over pure leaf like α-Fe_2O_3, which because reduced graphene oxide worked as the good adsorbent and electron acceptor to efficiently enhance the pollutant photodecomposition.

Keywords: **Leaf like α-Fe_2O_3; Reduced graphene oxide; Hydrothermal; Brilliant green, Acetophenone; Photocatalytic activity;**

I. INTRODUCTION

Nowadays with the huge development of different industries, environmental pollution, energy shortage and global warming challenges have attracted much intensive research interest worldwide. Solar energy conversion for environmental applications has received much attention in recent years [1, 2]. Heterogeneous photocatalysis has been extensively used for wastewater treatment and air purification [1–3]. In fact, photocatalysis can greatly contribute to the remediation of those environmental pollutants into environmental friendly species: CO_2, H_2O, etc [4, 5]. Semiconductor metal oxides, in particular, have been widely used as photocatalysts for the decomposition of organic pollutants, and air contaminants because of their high stabilities, redox capacities, low toxicities, and photo physical properties [6–8]. Fe_2O_3(Band gap 1.9 –2.2 eV) is one of the desirable semiconductor materials for photocatalytic applications because of its useful properties, including absorption in the visible range of the solar spectrum, high stability, low cost, and ready availability [9, 10]. However, the charge carrier recombination lowers its efficiency, which alternately limits the photocatalytic performance. In order to overcome these limitations, the focus of recent research has turned into the preparation of composite or hybrid materials for visible light photocatalytic applications [11, 12].

Another effective approach for improving the performance of semiconductor photocatalyst is the use of carbon materials as a composite which shows an effective electron transfer reactions. In this scenario, two-dimensional carbon materials like activated carbon, graphene-oxide (GO), graphene and graphdiyne are used as a carbon additive in the semiconductor photocatalysis [13, 14]. Amongst, graphene sheets have received much attention for developing composite materials for photocatalyst due to its exceptional electrical, thermal, mechanical properties, high theoretical surface area of up to 2630

International Journal of Engineering Applied Sciences and Technology, 2016
Vol. 1, Issue 10, ISSN No. 2455-2143, Pages 103-109
Published Online August - September 2016 in IJEAST (http://www.ijeast.com)



m^2 g^{-1} and their ability to anchor guest molecules on its basal planes via guest-host interaction [15].

Parida et al. [16] reported that α-Fe_2O_3 nanorods/reduced graphene oxide (RGO) composites showed relatively enhanced photocatalytic efficiency for phenol degradation and Li et al. [17] reported the photodegradation of toluene over a spindle-shaped α-Fe_2O_3 /graphene composite improved due to the fast transfer of photogenerated electrons from α-Fe_2O_3 to the rGO sheets. These renewed efforts revealed that α-Fe_2O_3/graphene composites were truly different from other α-Fe_2O_3/carbon composites on enhancement of photocatalytic activity for the degradation of organic pollutants and dyes.

In this present work, we report the leaf like α-Fe_2O_3/rGO composite with good distribution are synthesized for the first time using a simple one-step template-free hydrothermal method and the photocatalytic property of rGO supported leaf like α-Fe_2O_3 composite for degrading Brilliant green and Acetophonone. It is demonstrated that the leaf like α-Fe_2O_3/reduced graphene oxide exhibited enhanced photo activity in terms of visible light irradiation, when compared to pure leaf like α-Fe_2O_3 counterpart as in degrading the Brilliant green and Acetophonone.

II. EXPERIMENTAL SECTION

2.1. Synthesis of Graphene Oxide

Graphene Oxide(GO) was prepared by a modified Hummers method [18]. In a typical synthesis, 92 mL of sulfuric acid (98%) was taken in a 500 mL conical flask, which was kept in a ice bath. 2.0 g of graphite powders and 2.0 g of $NaNO_3$ were added to the above solution. 6.0 g of potassium permanganate was slowly added to the mixture and continuously stirred for 2 h at room temperature. To the above mixture 92 mL of deionized water was slowly added. A suitable amount of hydrogen peroxide (30%) was added it. Finally the mixture was filtered and washed with 5% HCl and deionized water until no sulfate ions in the filtrate was detected, the solid was dried at 70 ^oC in a oven for 24 hr.

2.2. Synthesis of leaf like α-Fe_2O_3

In a typical synthesis of leaf like α-Fe_2O_3(FO) [19], $K_3[Fe(CN)_6]$ was dissolved in distilled water to form a clear solution with a concentration of 0.1 mol/L, which was placed in a Teflon-sealed autoclave and maintained at a temperature of 140 ^oC for 2 days. The red product was isolated by centrifugation, repeatedly washed with distilled water and absolute ethanol, and dried at 60 ^{o} C in oven.

2.3. Synthesis of leaf-like α-Fe_2O_3-rGO composite

In a typical synthesis of leaf like α-Fe_2O_3-rGO (GFO), $K_3[Fe(CN)_6]$ was dissolved in distilled water to form a clear solution with a concentration of 0.1 mol/L and required amount of graphene oxide was added into the solution, the mixture solution continues sonicated 1 hr and then solution was transfer to Teflon-sealed autoclave and maintained at a temperature of 140 ^oC for 2 days. The red product was isolated by centrifugation, repeatedly washed with distilled water and absolute ethanol, and dried at 70 ^oC in oven. Obtained product calcinations at 300 ^oC 6 hr.

2.4. Characterizations

The crystal structures of the samples were analyzed on X-ray Diffractometer (XRD), using graphite monochromatized Cu Kα radiation. The XRD patterns were obtained in the range of 5^o–80° (2θ) at a scanning rate of 5° min^{-1}. Fourier Transform Infrared (FTIR) spectra were recorded on a FTIR analyzer. The samples were characterized on a Scanning Electron Microscope (SEM) with an acceleration voltage of 15 keV. The samples were coated with a 5 nm thick gold layer before the observations. Energy Dispersive X-ray (EDX) spectroscopy was used to measure the elemental analysis of prepared sample. The Thermogravimetric Analysis (TGA) was carried out on a TGA instrument from room temperature to 800 ^oC at a heating rate of 10 ^oC min^{-1} in air. UV-vis/DRS spectrophotometer (UV-vis / DRS) was used to measure the spectra in the region of 200 to 800 nm. The surface areas of the samples were calculated by the Brunauer–Emmett– Teller (BET).

2.5. Photocatalytic performance study of FO and GFO composite

The photocatalytic activities of the catalysts were evaluated by the degradation reactions of the Brilliant green (BG) dye (10 mg L^{-1}) and Acetophenone (AP) organic pollutant (15 mg L^{-1}) solutions. All the reactions were performed at room temperature and normal atmospheric pressure. Typically, 100 mg of the catalyst were suspended in 100 mL sample solution in a 150 mL beaker. Prior to irradiation, the system was placed in a total dark environment and magnetically stirred for 30 mints until adsorption-desorption equilibrium was reached. Following this, the photocatalytic reaction was started by the

International Journal of Engineering Applied Sciences and Technology, 2016
Vol. 1, Issue 10, ISSN No. 2455-2143, Pages 103-109
Published Online August - September 2016 in IJEAST (http://www.ijeast.com)

exposure of visible light. A certain mixture solution was taken out at regular intervals and centrifuged to remove the catalyst. The concentration of the dye was determined by using a UV-vis spectrophotometer.

The photometric analysis of the all photocatalyst samples before and after irradiation can be used by measuring % of degradation (Degradation efficiency (D_o)). Defined the following expression, where C_0 is the initial concentration of dye and C_t is the concentration of dye after irradiation of the samples in desired time intervals. All samples were conducted under the same experimental conditions.

$$\% \text{ of degradation} = \frac{Co - Ct}{Co} \times 100 \quad (1)$$

III. RESULTS AND DISCUSSIONS

3.1. XRD analysis

The XRD patterns of GO, FO, GFO are shown in Fig 1. Fig1(a) shows diffraction peaks at 2θ = 11 ° and 2θ = 43°, corresponding to the (002) and (100) reflections, respectively, of GO [20, 21]. Fig 1(b) shows diffraction peaks at 2θ = 24.2°, 33.1°, 35.7°, 40.9°, 49.4°, 54.2°, 57.6°, 62.4°, 64.0°, 69.6°, 72.0° and 75.5° assigned to the (012), (104), (110), (113), (024), (116), (122), (214), (300), (208), (101) and (220) diffraction planes respectively (JCPDS, no. 33-0664), which are attributed to Pure FO [22]. No other impurity peaks appear for pure FO, indicating the high purity of the as-prepared sample. The XRD analysis (Fig 1(c)) shows that the main diffraction peaks of the GFO composite similar to those of pure FO, indicating that the presence of rGO doesn't result in the development of new crystal orientations or changes in preferential orientations of FO. No typical diffraction peaks of carbon species are observed in the GFO composite, which may be due to the low amount and relatively low diffraction intensity of rGO, which is similar to those reported in the literatures [23, 24].

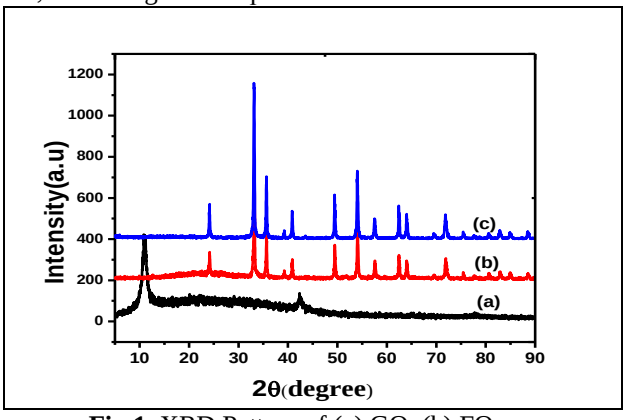


Fig 1. XRD Pattern of (a) GO, (b) FO and (c) GFO.

3.2. FTIR analysis

In Fig 2 exhibit the FTIR spectra of GO and GFO composite. GO and GFO composite both showed the O-H stretching vibration adsorption peak at 3000−3700 cm^{-1}. The obvious characteristic peaks of GO can be show in GO curve, the peaks at 1716 and 1390 cm^{-1} were the C=O stretching vibration peaks of carboxyl and carbonyl; the peak at 1581 cm^{-1} was attributed to the stretching vibration of aromatic C=C; the peaks at 1170 and 1033 cm^{-1} were ascribed to the C-O stretching vibration of epoxy and alkoxy groups [25]. These peaks demonstrated the existence of carboxyl, epoxy and alkoxy group in graphene oxide. GFO composite observed in GFO curve, after hydrothermal treatment, the Fe-O characteristic stretching vibration peak at 514 cm^{-1} for metal oxide and reaming peaks C=O disappears and the peak intensity of O−H and C−O decreases, which indicates the removal of oxygen-containing functional groups and the partial reduction of GO, leading to the formation of reduced graphene oxide (rGO) in the composite [26, 27] which proved that FO was successfully anchored onto rGO layer.

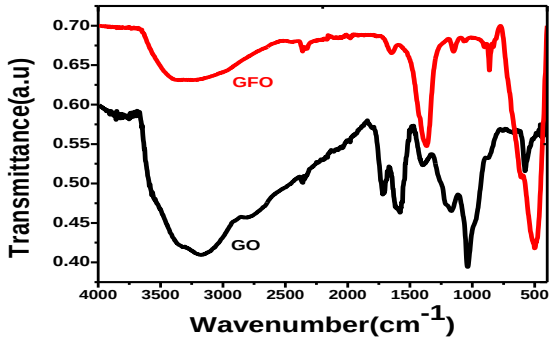


Fig 2. FTIR spectra of GO and GFO.

3.3. SEM - EDX analysis

Structure and Morphological features of different samples were examined by scanning electron microscopy (SEM) and the corresponding images are shown in Fig 3(a) and 3(b) shows pure FO leaf like structure. Fig 3(c) and 3(d) shows FO leafs are well-decorated on the surface of the rGO sheets. Here, by the introduction of FO leafs, the rGO sheets are

International Journal of Engineering Applied Sciences and Technology, 2016
Vol. 1, Issue 10, ISSN No. 2455-2143, Pages 103-109
Published Online August - September 2016 in IJEAST (http://www.ijeast.com)

exfoliated and intact with the FO leafs providing a composite material. The composition of the composite was determined from different regions using EDX spectroscopy. The corresponding EDX spectra (Fig 3(f)) peaks showed the presence of Fe, O and C. The absence of any other peak suggests that the composite is free from impurities. Composite contained 64.91 wt% Fe, 30.46 wt% O and 4.63 wt% C. The morphology and EDX analysis were in support of the XRD results which confirm the purity of composite structure.

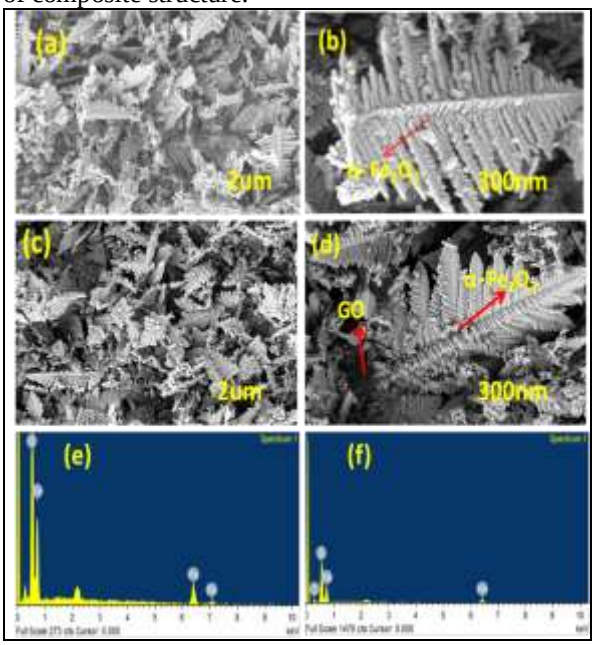


Fig 3. (a),(b) SEM images of FO (c),(d) SEM images of GFO (e), (f) EDX pattern of FO and GFO

3.4. TGA analysis

In order to perform a quantitative analysis of the photocatalyst TGA was applied. The samples were heated under air flow with the heating rate of 10 ^{o}C/min. The TGA curves of GFO are presented in Fig 4. Mass loss between 25 to 200 ^{o}C which is related to the evaporation of adsorbed water on composite, mass loss between 200 to 350 ^{o}C which is related to the removal of oxygen-containing functional groups. A significant mass loss was observed at the temperature range between 350 and 800 ^{o}C for this happened due to the pyrolysis of carbon skeleton [28]. Very low mass loss at the temperature range between 350 ^{o}C and 800 ^{o}C which confirms a successful reduction of GO into rGO during the calcinations.

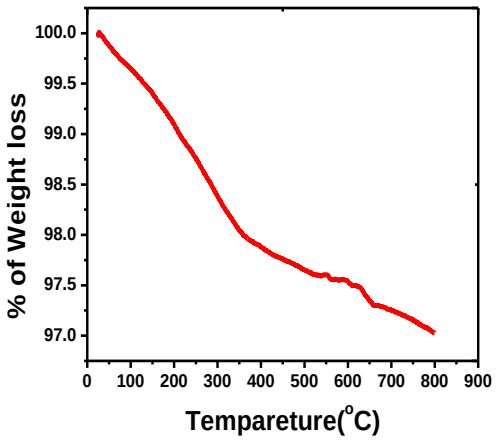


Fig 4. TGA spectra of GFO

3.5. UV- vis/DRS analysis

UV−vis/DRS spectra has been taken using UV−vis/DRS spectrophotometer. Fig 5 shows the DRS spectra of the synthesized FO and GFO. The UV−visible absorption spectra of FO show an absorption band at 625 nm. Whereas, in case of GFO absorption band at 670 nm [29]. GFO also shows an increase in the absorption spectra intensity in the visible light region compared to FO. This is due to the presence of blackbody properties of rGO. That means that the deoxygenated surface of GO is obtained during the composite formation by hydrothermal treatment, which indicates the conversion of GO to rGO. These interpretations also suggest that the presence of rGO indirectly modifies the fundamental process of electron−hole pair formation of by increasing its surface electric charge during the photochemical process. The band gap energies of FO, GFO are 1.90 eV, 1.85 eV respectively. As evidenced from the band-gap energies the introduction of rGO does not strongly affect the optical absorption property of FO, whereas its presence shifts the absorption edge of composite toward the red region.

The BET specific surface area of the GFO and FO samples have been determined those are 75.5 and 20.60 m^2 g^{-1}, respectively. It shows that the rGO constituent makes the specific surface area of the sample increase a lot. These features determining the accessibility of reactant molecules are important for the catalytic performance, which implies that the GFO composite may have higher photocatalytic activity than the FO.

International Journal of Engineering Applied Sciences and Technology, 2016
Vol. 1, Issue 10, ISSN No. 2455-2143, Pages 103-109
Published Online August - September 2016 in IJEAST (http://www.ijeast.com)

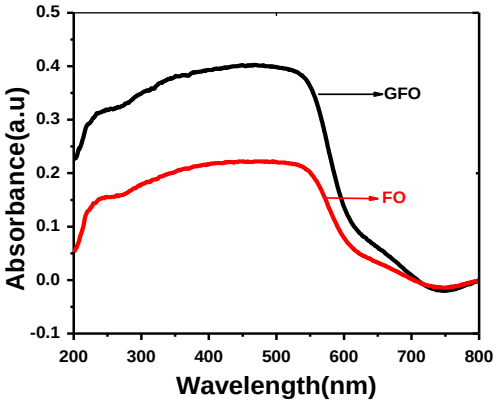


Fig 5. UV-vis DRS spectra of FO and GFO

3.6. Photocatalytic activity of FO and GFO

All the above results shows the GFO exhibit a wider absorption band between 400 nm and 800 nm and better surface area compared to that of pure FO [30, 31], Due to that as prepared composite exhibits considerably stronger photo response in the entire visible light region, which is favorable for utilizing more solar energy and improving photocatalytic activity [32–35]. The photocatalytic activities of the as prepared catalysts were evaluated by photodegradation experiments of the organic dye BG (λ=*625* nm) and organic pollutant AP (λ = 245 nm) in aqueous solutions under visible light irradiation. The results are displayed in Fig 6.

150 mL beaker containing 100 mL of BG (10 ppm) or 100 mL of AP (15 ppm) and catalyst (100 mg) were magnetically stirred for 30 min in the dark in order to establish an adsorption-desorption equilibrium. Following this, the photocatalytic reaction was started by the exposure of visible light. A 5 mL of mixture solution was taken out at regular intervals and centrifuged to remove the catalyst. The concentration of the sample was determined by using a UV-vis spectrophotometer. Fig 6(A) and 6(B) reveals the temporal evolution of the UV-visible absorption spectra of BG degraded over the FO and GFO composite. Under visible light irradiation, the color of the BG solution changed from initial Green to light Green and then disappeared green color during the reaction. Similar photocatalytic activity of Fig 6(C) and 6(D) results are get on GFO composite compared to FO for AP decomposition.

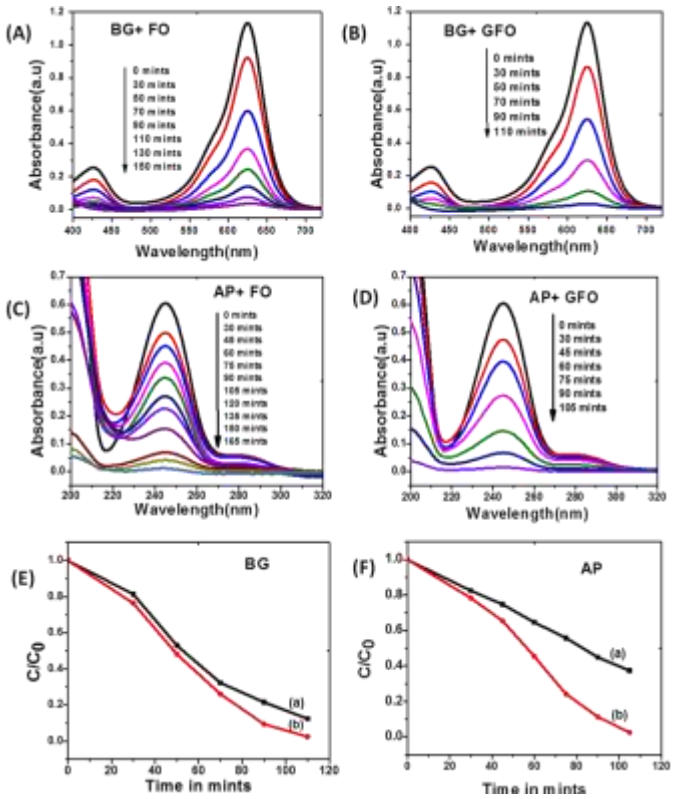


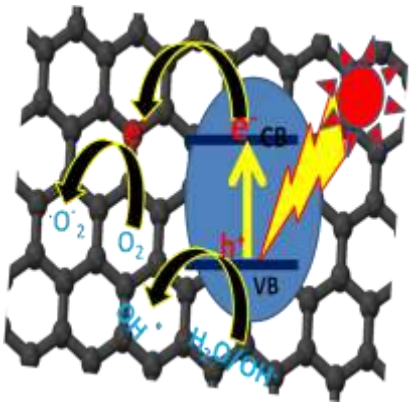
Fig 6. (A), (B) UV-visible absorption spectra of degradation of BG by FO and GFO under visible light. (C), (D) UV-visible absorption spectra of degradation of AP by FO and GFO under visible light. Photocatalytic degradation of (E) BG and (F) AP using FO and GFO under visible light.

For convenience, we assumed that the concentration of BG after desorption–adsorption equilibrium was the initial concentration C_0, the absorption peak at 625 nm drops gradually with increasing irradiation time and almost disappears after 110 min. Fig 6(E) shows the effects of visible light irradiation time (t) on the normalized BG concentration (C_t/C_0) for the BG aqueous solutions containing both catalysts. After irradiation of 110 min, the photocatalytic degradation efficiency (D_o) was calculated and the efficiency is 87.72 and 97.61% for FO and GFO respectively. And Fig 6(F) shows the effects of visible light irradiation time(t) on the normalized AP concentration (C_t/C_0) for the AP aqueous solution containing both catalysts. After irradiation of 105 min, the photocatalytic degradation efficiency (D_o) was calculated by Eq.1 and the efficiency is 62.64 and 97.52% for FO and GFO respectively. From these results, it is seen that

the exhibited high degradation efficiency. After irradiation of 120 min, the photocatalytic degradation efficiency was calculated by Eq.1 and the efficiency is 62.64% and 97.52% for FO and GFO respectively. From these results, it is seen that the GFO composite exhibited excellent photocatalytic activity compared to FO for BG and AP decomposition under visible light irradiation.

3.7. Photocatalytic mechanism

Based on the experimental results, a possible mechanism was proposed for photocatalytic performance of composite.



Scheme 1. The mechanism illustration of photocatalytic activity for GFO composite

Scheme1, The electrons in the valence band can be excited to the conduction band with the same amount of positively charged holes left to form electron-hole pairs when the UV-vis light irradiates, the electrons can then be transferred to the surface of rGO. The effective charge transfer can decrease the electron-hole pair recombination rate and prolong the lifetime of charge carriers, which increases the photocatalytic efficiency. The photo induced electrons are react with absorbed O_2 to form superoxide anion radical ($\bullet O_2^-$), while the holes could also react with surface-bound H_2O and OH^- to produce hydroxyl radicals (•OH). It is evident that hydroxyl radicals were the main active species for the degradation of pollutants [36, 37].

IV. CONCLUSION

In summary, leaf like α-Fe_2O_3-rGO composite was synthesized via a simple one-step hydrothermal method. The composites were well characterized by different instrumental techniques and the results were correlated. The possible growth of FO onto rGO layer led to a higher absorbance capacity for visible light by GFO composite than FO. The Photocatalytic activity of prepared GFO composite show good photocatalytic activity toward the degradation of BG and AP pollutants under irradiation of visible light compare to FO. It is possible for the highly efficient leaf like α-Fe_2O_3-rGO composite photocatalyst to be used to remove harmful pollutants in wastewater.

V. REFERENCES

[1] P. Luan, M. Xie, D. Liu, X. Fu and L. Jing, *Sci. Rep.*,4, 6180, 2014.
[2] X. B. Chen, S. H. Shen, L. J. Guo and S. S. Mao, *Chem. Rev.*,110, 6503–6570, 2010.
[3] F. Amano, K. Nogami and B. Ohtani, *J. Phys. Chem. C.*,113, 1536–1542, 2009.
[4] Sakthivel S, Shankar MV, Palanichamy M, Arabindoo B, Bahnemann DW, Urugesan V, *Water Res.*, 38, 3001-3008, 2005.
[5] Brijesh P, Pardeep S, Jonnalagadda SB, *Int. J. Chem.*,47,830-835,2008.
[6] P. V. Kamat, J. Phys. Chem. C, 111, 2834–2860, 2007.
[7] S. Dong, J. Feng, M. Fan, Y. Pi, L. Hu, X. Han, M. Liu, *J. Sun and J. Sun, RSC Adv.*,5,14610–14630, 2015.
[8] K. Rajeshwara, M. E. Osugi, W. Chanmanee, C. R.Chenthamarakshan, M. V. B. Zanoni, P. Kajitvichyanukul and R. Krishnan-Ayer, *J. Photochem. Photobiol.C.*, 9, 171–192, 2008.
[9] D. K. Zhong, J. Sun, H. Inumaru and D. R. Gamelin., *J. Am. Chem. Soc.*, 131, 6086– 6087, 2009.
[10] Y. J. Lin, G. B. Yuan, S. Sheehan, S. Zhou and D. W. Wang., *Energy Environ. Sci.*,4, 4862–4869, 2011.
[11] J.J. Macías-S_anchez, L. Hinojosa-Reyes, A. Caballero-Quintero, W. de la Cruz,E. Ruiz-Ruiz, A.Hern_andez-Ramírez, et al., *Photochem. Photobiol. Sci.*,14, 536-542, 2015.
[12] S. Xu, L. Fu, T.S.H. Pham, A. Yu, F. Han, L. Chen, *Ceram. Int.*, 41,4007-4013, 2015.
[13] A. Mills, C.O. Rourke, K. Moore, *J. Photochem. Photobio. A. Chem.*, 310, 66-105, 2015.
[14] T. Sakthivel, K. Karthikeyan, K. Velmurugan, R. Nandhakumar, S.-J. Kim, V. Gunasekaran, J. Phys. Chem. C., 119 150911094658005, 2015.
[15] G.K. Veerasubramani, K. Krishnamoorthy, S.J. Kim, *RSC Adv.*, 5, 16319-16327, 2015.
[16] G. K. Pradhan , D. K. Padhi , K. Parida , *ACS*



Appl. Mater. Interfaces., 5 , 9101-10, 2013 .
[17] H. Li , Q. Zhao , X. Li , Z. Zhu , M. Tade , S. Liu , *J. Nanoparticle Res., 15* , 1, 2013.
[18] W.S. Hummers, R.E. Offeman, *J. Am. Chem. Soc.*, 80, 1339-1339, 1958.
[19] Genban Sun,*,† Bingxiang Dong,† Minhua Cao,*,‡ Bingqing Wei,*, and Changwen Hu, *Chem. Mater.*,23, 1587–1593, 2011.
[20] Y. Zhao, X. Song, Q. Song and Z. Yin, *CrystEngComm.*,14, 6710–6719,2012.
[21] H. Feng, Y. Li and J. Li, *RSC Adv.*, 2, 6988–6993, 2012.
[22] S.B. Wang, W. Wang, P. Zhan, S.Q. Jiao, ChemElectroChem.,1, 1636–1639, 2014.
[23] X.J. Liu, L.K. Pan, T. Lv, G. Zhu, T. Lu, Z. Sun, C.Q. Sun, RSC Adv., 1, 1245–1249, 2011.
[24] Xinjuan Liu , Taiqiang Chen , Haipeng Chu , Lengyuan Niu , Zhuo Sun ,Likun Pan , Chang Q. Sun, *Electrochimica Acta.*, 166, 12–16, 2015.
[25] V. Chandra, J. Park, Y. Chun, J.W. Lee, I.C. Hwang, K.S. Kim, *ACS Nano.*, 4, 3979–3986, 2010.
[26] Fu, Y. S.; Wang, X. *Ind. Eng. Chem. Res.*, 50, 7210-7218, 2011.
[27] Cui, C.; Wang, Y. P.; Liang, D. Y.; Cui, W.; Hu, H. H.; Lu, B. Q.; Xu, S.; Li, X. Y.; Wang, C.; Yang, Y. *Appl. Catal .B.*,150 ,158-159, 2014.
[28] Jeong H.K., Lee Y.P., Jin M.H., Kim E.S., Bae J.J., Lee Y.H.,*Chem. Phys. Lett.*, 470, 255-258, 2009.
[29] Cornell, R. M.; Schwertmann, U. The Iron Oxide Book, 2nd ed.; *Wiley-VCH: Weinheim, Germany.*, p 147, 2003.
[30] W. S. Wang, H. Du, R. X. Wang, T. Wen and A. W. Xu, *Nanoscale.RSC.*, 5, 3315, 2013.
[31] G. P. Dai, J. G. Yu and G. Liu, *J. Phys. Chem. C*, 116, 15519-15524, 2012.
[32] Y. X. Yang, W. Guo, Y. N. Guo, Y. H. Zhao, X. Yuan and Y. H. Guo, *J. Hazard. Mater.*, 271, 150-159, 2014.
[33] P. Wang, B. B. Huang, Y. Dai and M. H. Whangbo, *Phys. Chem. Chem. Phys.*, 14, 9813-9825, 2012.
[34] Y. L. Min, G. Q. He, Q. J. Xu and Y. C. Chen, *J. Mater. Chem. A*, 2, 1294, 2014.
[35] Q. Zhu, W. S. Wang, L. Lin, G. Q. Gao, H. L. Guo, H. Du and A. W. Xu, *J. Phys. Chem. C.*, 117, 5894-5900, 2013.
[36] D. Lin , H. Wu , R. Zhang , W. Pan , *Chem. Mater. 21* , 3479-3484, 2009**.**
[37] S. C. Han , L. F. Hu, N. Gao , A. A. Al-Ghamdi, X. S. Fang , *Adv. Funct. Mater. 24* , 3725, 2014**.**

IJEAST

INTERNATIONAL JOURNAL
OF ENGINEERING APPLIED SCIENCE AND TECHNOLOGY

AUTHORS

- Balaji Anjaneyulu Rachuri
- Parasuram Naidu Gongada
- Muralikrishna Rallabhandi
- Sathish Mohan Botsa

ABOUT IJEAST

International journal of Engineering Applied Science and Technology (IJEAST) is a peer-reviewed, open access journal that publishes high - quality research paper in the field of Engineering, Applied Science and Technology.

IJEAST aims to provide a platform for researchers, academicians, and professionals to share their innovative ideas, research findings, and practical experiences with the global scientific community.

JOURNAL METRICS

H-INDEX	i10-INDEX	IJEAST CITATIONS	PEER-REVIEWED & OPEN ACCESS
33	154	9,647 (IJEAST CITATIONS)	PUBLISHED MONTHLY

PEER REVIEWED

All submission are rigorously peer reviewed to ensure quality.

AUTHORS ARE OUR PRIORITY

We value our authors and recognize their contribution to the advancement of research and knowledge.

OPEN ACCESS

Free and unrestricted access to research for all.

GLOBAL REACH

Connecting researchers and professionals worldwide.

TIMELY PUBLICATION

We ensure a swift and efficient publication process.

For more information, visit our website
www.ijeast.com

editor@ijeast.com
www.ijeast.com
India

2455-2143